

## Simultaneous PKC and cAMP activation induces differentiation of human dental pulp stem cells into functionally active neurons

Marianna Király<sup>a</sup>, Balázs Porcsalmy<sup>a</sup>, Ágnes Pataki<sup>b</sup>, Kristóf Kádár<sup>a</sup>, Márta Jelitai<sup>c</sup>, Bálint Molnár<sup>a,e</sup>, Péter Hermann<sup>d</sup>, István Gera<sup>e</sup>, Wolf-Dieter Grimm<sup>f</sup>, Bernhard Ganss<sup>g</sup>, Ákos Zsembery<sup>b</sup>, Gábor Varga<sup>a,\*</sup>

<sup>a</sup> Department of Oral Biology, Semmelweis University, Budapest, Hungary

<sup>b</sup> Institute of Human Physiology and Experimental Research, Semmelweis University, Budapest, Hungary

<sup>c</sup> Institute of Experimental Medicine, Hungarian Academy of Sciences, Budapest, Hungary

<sup>d</sup> Department of Prosthodontics, Semmelweis University, Budapest, Hungary

<sup>e</sup> Department of Periodontology, Semmelweis University, Budapest, Hungary

<sup>f</sup> Department of Periodontology, University of Witten-Herdecke, Germany

<sup>g</sup> CHIR Group in Matrix Dynamics, University of Toronto, Canada

### ARTICLE INFO

#### Article history:

Received 27 March 2009

Accepted 30 March 2009

Available online 5 April 2009

#### Keywords:

Dental pulp

Stem cell

Neuronal differentiation

Human

Electrophysiology

Patch clamp

Voltage-dependent sodium channel

Voltage-dependent potassium channel

Immunocytochemistry

Cell culture

### ABSTRACT

The plasticity of dental pulp stem cells (DPSCs) has been demonstrated by several studies showing that they appear to self-maintain through several passages, giving rise to a variety of cells. The aim of the present study was to differentiate DPSCs to mature neuronal cells showing functional evidence of voltage gated ion channel activities *in vitro*. First, DPSC cultures were seeded on poly-L-lysine coated surfaces and pretreated for 48 h with a medium containing basic fibroblast growth factor and the demethylating agent 5-azacytidine. Then neural induction was performed by the simultaneous activation of protein kinase C and the cyclic adenosine monophosphate pathway. Finally, maturation of the induced cells was achieved by continuous treatment with neurotrophin-3, dibutyryl cyclic AMP, and other supplementary components. Non-induced DPSCs already expressed vimentin, nestin, N-tubulin, neurogenin-2 and neurofilament-M. The inductive treatment resulted in decreased vimentin, nestin, N-tubulin and increased neurogenin-2, neuron-specific enolase, neurofilament-M and glial fibrillary acidic protein expression. By the end of the maturation period, all investigated genes were expressed at higher levels than in undifferentiated controls except vimentin and nestin. Patch clamp analysis revealed the functional activity of both voltage-dependent sodium and potassium channels in the differentiated cells. Our results demonstrate that although most surviving cells show neuronal morphology and express neuronal markers, there is a functional heterogeneity among the differentiated cells obtained by the *in vitro* differentiation protocol described herein. Nevertheless, this study clearly indicates that the dental pulp contains a cell population that is capable of neural commitment by our three step neuroinductive protocol.

© 2009 Elsevier Ltd. All rights reserved.

### 1. Introduction

One of the first signs of mammalian tooth development is seen as the oral epithelium starts to invaginate into the underlying neural crest-derived mesenchyme. The mesenchymal cells are derived from the dorsal-most aspect of the neural tube, and contribute to many tissues, including the dental pulp (Thesleff and Aberg, 1999; Tucker and Sharpe, 2004). From this aspect, it would be of great interest to identify a neural progenitor pool in the adult human dental tissues, and investigate its regenerative potential for

nervous system defects such as neurodegenerative diseases or disorders arising from stroke or injuries.

Dental pulp harbors a subset of cells that are able to differentiate along several pathways, including neural and mesenchymal progenitors (Arthur et al., 2008; d'Aquino et al., 2007; Gronthos et al., 2000; Koyama et al., 2009; Miura et al., 2003; Nosrat et al., 2004; Shi et al., 2005). Both neural and mesenchymal progenitors have been shown to have the potential for neurogenesis similar to that of embryonic stem cells (Bouchez et al., 2008; Hamanoue et al., 2007; Kimiawada et al., 2009; Ma et al., 2007; Orojan et al., 2008; Rizvanov et al., 2008). Previous studies revealed that dental pulp stem cells (DPSCs), when transplanted into adult rat/mouse brain, infiltrated into the host nerve tissue, and expressed neurospecific markers (Miura et al., 2003; Nosrat et al., 2004). It was also reported, that dental-pulp odontoblasts

\* Corresponding author. Fax: +36 1 210 4421.

E-mail address: [varga-g@net.sote.hu](mailto:varga-g@net.sote.hu) (G. Varga).

show some partial neuronal-like features (Pavlin et al., 1991; Pavlin and Vidmar, 1979) to enable their sensory function (Allard et al., 2006; Magloire et al., 2003, 2008). Very recently a pioneer study demonstrated that DPSCs can be differentiated into neuronal-like cells in Neurobasal media supplemented with differentiation factors (Arthur et al., 2008). That protocol, however, resulted in an incomplete neuronal differentiation, since only voltage gated sodium channels could be detected without the presence of voltage gated potassium channels which are also regarded as a basic criterion for functional neuronal cell identification (Arthur et al., 2008).

It has been known for some time that activation of the cAMP and PKC signaling pathways promotes neuron and glia differentiation (Audesirk et al., 1997; Cabell and Audesirk, 1993; Iacovitti et al., 2001; Kim et al., 2002; Otte et al., 1989). Human bone marrow stromal stem cells (BMSCs) were also shown to differentiate into neural progenitors in response to PKC activation and increased intracellular cAMP level (Deng et al., 2001; Scintu et al., 2006). However, these changes were transient, and the cells reverted to the original fibroblastic BMSCs within 48 h (Scintu et al., 2006). Factors that elevate intracellular cAMP induce neuroendocrine differentiation in cell lines of diverse origins (Bang et al., 1994; Ghosh and Singh, 1997; Moore et al., 1996; Sharma and Raj, 1987). Moreover, a number of previous studies demonstrated the importance and necessity of neuronal differentiation factors such as neurotrophin-3 (NT-3) and nerve growth factor (NGF) during neuronal maturation. Furthermore, bFGF, EGF and retinoic acid were also reported to be regulators of cell proliferation and neural commitment (Arthur et al., 2008; Tataru et al., 2007; Wiedera et al., 2007). DNA methylation may promote cell differentiation by preventing transcriptional regulator proteins binding to the appropriate sequences, and by recruiting additional chromatin remodeling proteins forming compact, inactive silent chromatin. 5-Azacytidine has been shown to cause hemi-demethylation of DNA (Holliday, 1996), leading to dedifferentiation of partly committed cells to a multipotent state. It was also reported to be a potent maturation inducing factor for neurogenesis (Kohyama et al., 2001; Schinstine and Iacovitti, 1997).

In the present study, we investigated whether adult human DPSCs were capable of producing a large number of electrically active neural cells. Therefore, we developed a three step differentiation method involving: (1) *pretreatment* with 5-azacytidine and bFGF, (2) *induction* with bFGF, NGF, NT-3 and the consecutive stimulation of the PKC and cAMP pathways and (3) followed by *maturation* under increased cAMP, continuously added NT-3 and other neuroprotective factors. Our results demonstrate that using our protocol DPSCs can be differentiated into cells that not only express neuronal markers, but also display simultaneous voltage dependent sodium and potassium currents.

## 2. Experimental protocols

### 2.1. Materials

Alpha-modification of Eagle's medium ( $\alpha$ MEM), Neurobasal A medium, 1:1 ratio of Dulbecco's modified Eagle's medium (DMEM, Invitrogen) and F12 media (DMEM/F12), fetal calf serum (FCS), N2 and B27 supplements, penicillin and streptomycin were obtained from Invitrogen. Other standard reagents and cytokines were purchased from Sigma. Tissue culture dishes were from Costar. RNA isolation and purification kits (RNeasy Plus Micro Kit with on-column DNase digestion) were from Qiagen. Polyclonal anti-NF-M (neurofilament M), anti-GFAP (glial fibrillary acidic protein), and monoclonal anti-NeuN (neuronal nuclei) were purchased from Chemicon. Monoclonal anti-N-tubulin was from Santa Cruz.

### 2.2. Isolation and culture of human DPSCs

Normal impacted human third molars were collected from adults (19–55 years of age) at the Departments of Maxillofacial Surgery, Prosthodontics and Periodontology, Semmelweis University, Hungary, under approved guidelines set by the

National Institutes of Health Office of Human Subjects Research. Human DPSCs were isolated and cultured as previously reported (Gronthos et al., 2000). Briefly, dental pulp tissues were minced and then digested in a solution of 3 mg/ml collagenase type I and 4 mg/ml dispase type II for 1 h at 37 °C. After centrifugation, cells were resuspended in culture media, and passed through a 70  $\mu$ m strainer to obtain single-cell suspension. Cells were seeded in culture dishes and maintained under standard conditions (37 °C, 100% humidity, 5% CO<sub>2</sub>) in  $\alpha$ MEM medium, supplemented with 100  $\mu$ M ascorbic acid 2-phosphate, 2 mM L-glutamine, 100 U/ml penicillin, 100  $\mu$ g/ml streptomycin and 10% fetal calf serum (FCS). Subconfluent cultures were regularly passaged by treatment with 0.05% trypsin in phosphate-buffered saline (PBS, pH 7.4) and seeded at a density of 10<sup>4</sup> cells/cm<sup>2</sup>.

### 2.3. Osteogenic differentiation

Osteogenic differentiation was achieved as reported previously (Song and Tuan, 2004). Briefly, DPSCs were cultured with 1% FCS, 100 U/ml penicillin, 100  $\mu$ g/ml streptomycin, 2 mM L-glutamine, 10<sup>-8</sup> M dexamethazone, 50  $\mu$ g/ml L-ascorbic acid 2-phosphate, 10 mmol/l  $\beta$ -glycerophosphate in  $\alpha$ MEM for 20 days without passaging, but replacing the medium twice a week, after which calcium accumulation was detected by 2% Alizarin red S (pH 4.2, buffered with ammonium hydroxide) staining.

### 2.4. Neural differentiation

For neuronal induction, cultured morphologically homogeneous dental pulp cells (DPSC cultures, passage 1–4) were seeded at 20,000 cells/cm<sup>2</sup> in poly-L-lysine coated 10 cm Petri dishes, 6 well plates and coverslips in DMEM/F12 (1:1), 2.5% FCS, 100 U/ml penicillin, and 100  $\mu$ g/ml streptomycin, and cultured for 24 h. Epigenetic reprogramming (step 1) was performed using 10  $\mu$ M 5-azacytidine in DMEM/F12 containing 2.5% FCS and 10 ng/ml bFGF for 48 h. Neural differentiation (step 2) was induced by exposing the cells to 250  $\mu$ M IBMX, 50  $\mu$ M forskolin, 200 nM TPA, 1 mM dbcAMP, 10 ng/ml bFGF, 10 ng/ml NGF, 30 ng/ml NT-3, 1% of insulin-transferrin-sodium selenite premix (ITS) in DMEM/F12 for 3 days. At the end of the neural induction treatment, cells were washed with PBS, and then neuronal maturation (step 3) was performed by maintaining the cells in Neurobasal A media supplemented with 1 mM dbcAMP, 1% N2, 1% B27, and 30 ng/ml NT-3 for 3–7 days. All solutions were freshly prepared immediately prior to use. Following each step, cells in one well of the 6 well plates were lysed in lysis buffer containing 1%  $\beta$ -mercaptoethanol (Qiagen), and stored for RT-PCR analysis. After the final step, coverslips were fixed for immunocytochemistry analyses, or used for electrophysiological recordings.

### 2.5. MTT assay

To determine viable cell number in the cultures, an indirect method measuring metabolic activity of mitochondrial enzymes was used. The assay is based on the cellular conversion of a tetrazolium salt [MTT: 3-(4,5-dimethylthiazol-2-yl)2,5-diphenyltetrazolium bromide] to formazan. Control and treated cells were incubated with MTT (0.2 mg/ml) diluted in the appropriate media, in each phase of the differentiation for 60 min at 37 °C in 96-well plates. Culture medium was removed and formazan was solubilized in DMSO (100  $\mu$ l). The extent of reduction of MTT to formazan within cells was quantified by using a spectrophotometer (Bio-Rad 3550, Bio-Rad Laboratories) at a wavelength of 480 nm with the reference wavelength of 650 nm. Absorbance is directly proportional to the number of living cells in culture. Changes in cell viability were estimated by calculating the relative absorbance values normalized to absorbance values of the confluent culture from the same sample on each plate, which were used as internal controls (the cell number of the confluent grown wells on each plate remained constant 9500  $\pm$  380 cells/well during the 9 days long experiment series).

### 2.6. RT-PCR

Total RNA from DPSCs was isolated by lysis buffer supplemented with 1%  $\beta$ -mercaptoethanol and RNA was cleaned up using an RNeasy Plus Micro Kit (Qiagen) with on-column DNase digestion. The concentration of the RNA was determined by the Ribogreen method (Invitrogen). The integrity of the RNA was verified by electrophoresis on a 1% agarose gel and 200 ng total RNA was used per sample for cDNA synthesis, using random primers (High-Capacity cDNA Archive Kit, Applied Biosystems) in a total volume of 50  $\mu$ l. cDNA was subsequently amplified by polymerase chain reaction (PCR) using specific oligonucleotide primers and conditions described and successfully used previously.

PCR reactions were performed using the following primers and conditions after optimization using the gradient PCR method: vimentin (VIM) sense primer 5'-GGGACCTCTACGAGGAGGAG-3' (Scintu et al., 2006) and anti-sense primer 5'-CCGATTGCAACATCCTGTGC-3' (Scintu et al., 2006), 94 °C 30 s, 59 °C 30 s and 72 °C 30 s, 30 cycles; nestin (NES) sense primer 5'-GCCCTGACACTCCAGTTT-3' (Scintu et al., 2006) and anti-sense primer 5'-GGAGTCCTGGATTCCTCC-3' (Scintu et al., 2006), 94 °C 30 s, 55 °C 30 s and 72 °C 30 s, 33 cycles; neurogenin-2 (NGN2) sense primer 5'-GTCTCCCGGGATTTTGAT-3' and anti-sense primer 5'-TCTCCATCTGG-CAGAGCTT-3', 94 °C 30 s, 55 °C 60 s and 72 °C 90 s, 35 cycles; N-tubulin sense

primer 5'-ATGAGGGAGATCGTG-3' (Carles et al., 1999) and anti-sense primer 5'-AAAGGCCCTGAGCGGACT-3' (Carles et al., 1999), 94 °C 10 s, 59 °C 30 s and 72 °C 30 s, 33 cycles; NSE sense primer 5'-CATCGACAAGGCTGGCTACACG-3' (Hung et al., 2002) and anti-sense primer 5'-GACAGTTGACGGCTTTTCTTC-3' (Hung et al., 2002), 94 °C 60 s, 56 °C 60 s and 72 °C 120 s, 33 cycles; NF-M sense primer 5'-TGGGAAATGGCTCGTCAATT-3' (Scintu et al., 2006) and anti-sense primer 5'-CTTCATGGAACGGCCAA-3' (Scintu et al., 2006), 94 °C 30 s, 57 °C 60 s and 72 °C 90 s, 35 cycles; GFAP sense primer 5'-GCAGAGATGATGGAGCTCAATGACC-3' (Nagai et al., 2007) and anti-sense primer 5'-GTTTCATCTGGAGCTTCTGCCTCA-3' (Nagai et al., 2007), 94 °C 30 s, 55 °C 30 s and 60 °C 60 s, 35 cycles; 96 °C 10 s, 55 °C 20 s and 72 °C 40 s for  $\beta$ -actin. PCR reactions were performed with an Eppendorf Mastercycler gradient PCR machine.

### 2.7. Real-time PCR

For quantitative PCR amplification, 5% of the cDNA synthesis reaction was used with the real-time PCR primers and target-specific fluorescence probe (FAM-labeled MGB probe). The probes and primers were selected from the Applied Biosystem Assay on Demands database for the specific markers (VIM, NES, N-tub, NSE, NF-M, GFAP) and for the human acidic ribosomal phosphoprotein P0 (RPLP0), which was used as an internal control. Universal Mastermix (Roche Diagnostics) containing AMP-erase was used for amplification in a total volume of 20  $\mu$ l. For detection of fluorescence signal during the PCR cycles, a LightCycler 480 (Roche) was used with the default setting (50 °C for 2 min, 95 °C for 10 min, 45 cycles: 95 °C for 15 s, 60 °C for 1 min). Each treatment was repeated five times and each sample was measured in duplicate. Changes in gene expression levels were estimated by calculating the relative expression values normalized to the RPLP0 level from the same sample.

### 2.8. Immunocytochemistry

DPSCs grown on poly-L-lysine-coated glass coverslips were fixed with 4% PFA in PBS for 20 min at room temperature (RT), then permeabilized with 0.1% Triton X-100 (in PBS) for 8 min. To block non-specific binding, fixed cultures were incubated in PBS containing 4% bovine serum albumin (BSA; 90 min at RT), then reacted with primary antibodies at 4 °C overnight. Antibodies were diluted in 4% BSA as follows: anti-N-tub 1/200, NeuN 1/50, NF-M 1/200, and GFAP 1/1500. IgG anti-mouse and anti-rabbit Alexa fluor 488 conjugated (Molecular Probes) secondary antibodies were diluted 1/750 and applied for 1 h at RT. After washing, the preparations were mounted with Mowiol containing 10 mg/ml bisbenzimidazole (Hoechst 33258). Labeled sections were examined by fluorescent microscopy (Nikon Eclipse E600, Nikon Instruments), and images were captured with a cooled CCD camera (POT RT Color 2000, Diagnostic Instruments) connected to a PC running image acquisition software (SPOT Advanced, Diagnostic Instruments). The digitized images of DAPI and specific stainings were merged using Adobe Photoshop.

### 2.9. Patch-clamp recordings

Voltage-clamp recordings were performed using the whole-cell technique (Hamill et al., 1981) at room temperature with an Axopatch 200B amplifier (Axon Instruments). Micropipettes were fabricated by a P-97 Flaming/Brown type micropipette puller (Sutter Instrument) from GC120F-10 glass capillary tubes (Harvard Apparatus) and had a resistance of 5–10 M $\Omega$  when filled with pipette solution. Capacitive currents were compensated with analog compensation. Linear leak currents were not compensated. Series resistance was approximately 8–15 M $\Omega$ , and series resistance compensation (70–80%) was used in whole-cell recordings if the current exceeded 1 nA. Currents were filtered at 2 kHz (four-pole Bessel filter) and sampled at 5 kHz. Pulse generation, data acquisition, and analysis were performed using the pClamp 6.03 software (Axon Instruments). For whole-cell recordings, the electrodes were filled with a solution containing (in mM): KCl 130.0, CaCl<sub>2</sub> 0.5, MgCl<sub>2</sub> 2.0, EGTA 5.0 and HEPES 10.0 (pH 7.2). The extracellular solution contained (in mM): NaCl 145.0, KCl 3.0, CaCl<sub>2</sub> 2.0, MgCl<sub>2</sub> 1.0, D-glucose 10.0, HEPES 10.0, osmolality 300 mmol/kg, supplemented when appropriate with 1 mM tetrodotoxin (TTX, Alomone Diagnostics) or 5 mM tetraethyl ammonium chloride (TEA) (final concentrations).

### 2.10. Electrophysiological measurements and protocols

Electrophysiological measurements were performed according to a protocol described previously (Hamill et al., 1981) with minor modifications. Input resistance (IR) was determined from the currents elicited by a 10 mV test pulse depolarizing the cell membrane from  $-70$  to  $-60$  mV, 40 ms after the onset of depolarizing pulse. Membrane conductance was determined from currents elicited by depolarization from a holding potential of  $-70$  to  $+10$  mV. Currents were measured 40 ms after the onset of the pulses. Membrane capacitance (Cm) was estimated by using the time constant of the membrane, which was calculated by fitting the double-exponential function to the measured currents elicited by a 10 mV test pulse depolarizing the cell membrane from  $-70$  to  $-60$  mV (Schroder et al., 1999). Current patterns were obtained by clamping the cell membrane from a holding potential of  $-70$  mV to values ranging to  $+10$  mV at intervals of 10 mV.

Pulse duration was 50 ms. To isolate the voltage-gated K<sub>DR</sub> and TTX-sensitive Na<sup>+</sup> currents, the voltage step from  $-70$  to  $-60$  mV was used to subtract the time- and voltage-independent currents. The amplitudes of K<sub>DR</sub> were measured at the end of the pulse. Na<sup>+</sup> current amplitudes were measured at the peak value. The changes in current amplitudes were expressed as changes in current densities (pA/pF).

### 2.11. Statistical analysis

All values are expressed as mean  $\pm$  S.E.M. Statistical comparisons were performed in Sigma-Plot 10.0 software. The differences between groups were evaluated via one-way repeated measures of ANOVA followed by post hoc Dunnett tests.

## 3. Results

### 3.1. Isolation, culture, passage and osteogenic differentiation of DPSCs

Dental pulp stem cell cultures consist of morphologically homogenous, spindle-shaped cells, harboring elements that express stem cell and progenitor markers (Arthur et al., 2008; Laino et al., 2005; Shi and Gronthos, 2003). Following their release by enzymatic digestion from the host tissue, and cultivation under standard conditions, they adhere to the tissue culture grade plastic surface and start dividing (Fig. 1A and B). They expand even more rapidly than BMSCs (Gronthos et al., 2000). 2–3 weeks after plating, DPSCs isolated from a normal human impacted third molar reach confluence in a standard T75 culture dish (Fig. 1C and D).

Several recent studies reported that DPSCs were capable of osteogenic differentiation (d'Aquino et al., 2007; Gronthos et al., 2000). Under our experimental conditions, the cultures plated in parallel with those prepared for neuronal differentiation showed overt signs of mineralization by accumulating insoluble calcium deposits (Fig. 1E and F). Thus, this observation confirms the previous findings that DPSCs are capable of differentiation into at least two different cell types, which are normally derived from different germ layers.

### 3.2. Differentiation of dental pulp stem cells into a neuronal lineage

Dental pulp stem cells give rise to neuronal cells consistently and reproducibly when induced by activators of the PKC and cAMP signaling pathways. Non-induced cells (Fig. 2A, stage A) display flat morphology typical of fibroblasts, but become more rounded after pretreatment with 5-azacytidine and bFGF for 48 h (stage B). After 2 h of treatment with the inducing mixture, DPSCs grow processes and start moving towards the high cell-density areas (Fig. 2B, stage C). During the 3 days of induction, cells anchor their position in the network structure, the previously developed processes disappear, and their morphology reverts to flat and round cell shapes observed during earlier stages of differentiation (stage D). In the final maturation step, cells diverging radially from the centers begin to grow neurite-like processes (Fig. 2C, stage E). After 10 days of differentiation, the vast majority of cells display complex neuronal morphology, expressing both bipolar and stellate forms (Fig. 2D and E, stage F). However, a small portion of cells retain their flat shape, and are attached beneath the processes of the neuronal cells (Fig. 2D and E). These elements are presumably committed towards glial fates, or serve as a stanchion for the developing neuronal cells. Therefore, they might be indispensable for neuronal survival. Taken together, our three step differentiation procedure over 10 days results in a robust differentiation of cells towards neural lineages in essentially all surviving cells that initially showed all characteristics of dental fibroblasts. However, exclusion of the intracellular cAMP increasing components (dbcAMP, forskolin, IBMX, Fig. 2F) or the PKC activator TPA (Fig. 2G) from our differentiation protocol resulted in the development of incomplete neural-like morphology by the 10th day of the differentiation procedure. When we applied the recently

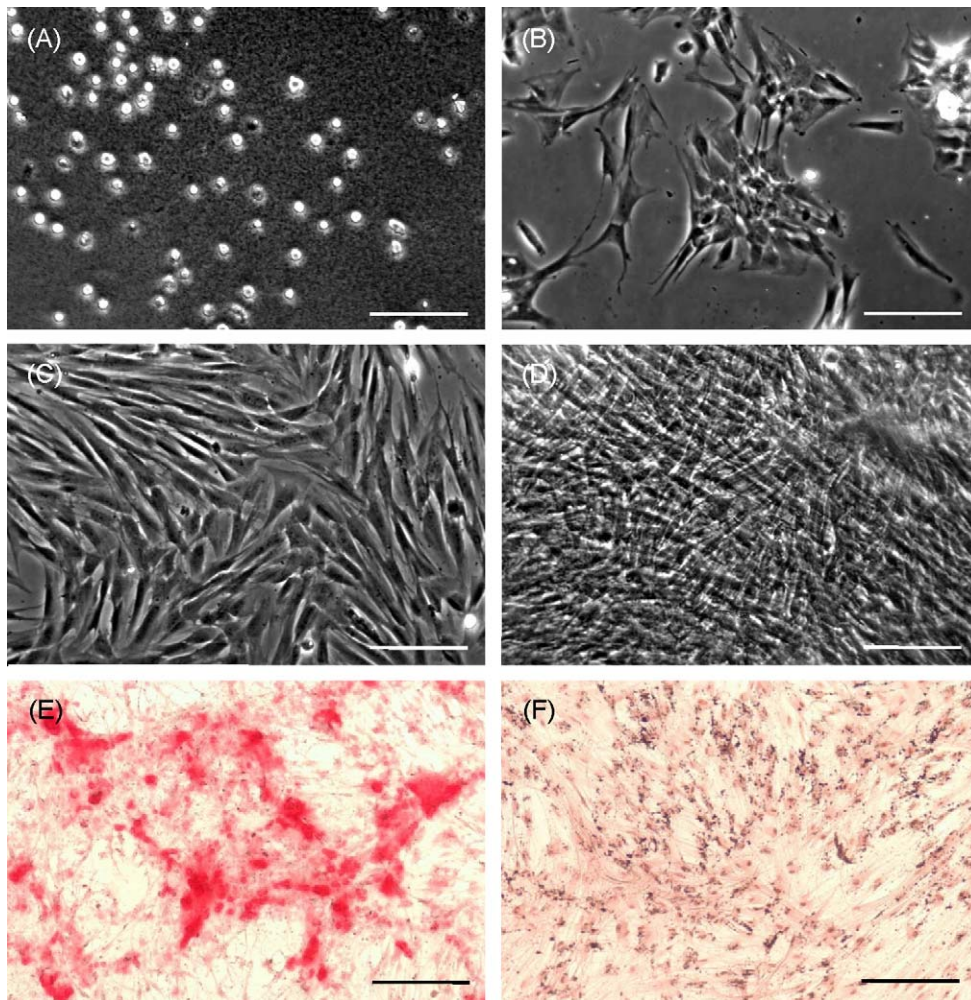


**Fig. 1.** DPSC (p2) cell morphology during culture, and osteogenic differentiation: (A) rounded DPSCs photographed before attaching to the plastic surface directly after isolation, (B) cells form colonies after 1 week in culture, (C) subconfluent culture after 3 weeks, (D) confluent DPSCs, (E) DPSCs produced mineralized deposits under osteogenic conditions as detected by 2% Alizarin Red S staining and (F) control staining of non-induced DPSCs. The lengths of the bars indicate 100  $\mu\text{m}$ .

described differentiation protocol for periodontal ligament-derived stem cells (Widera et al., 2007) (Fig. 2H), we found the formation of some neuronal-like structures, but the proportion of these cells compared to the entire population appeared to be very small, probably due to the high proliferation capacity of the overgrowing undifferentiated early passage DPSCs that we used in our studies. However, we also found that treatment with the combination of bFGF, EGF and retinoic acid (Widera et al., 2007) acts in a highly effective manner on the neural differentiation of stem cell cultures isolated from the human periodontal ligament (data not shown).

### 3.3. Cell viability profile during the differentiation process

Viability of human dental pulp stem cells during differentiation was evaluated by MTT assay (Fig. 3). Four DPSC cultures collected from different patients were used for cell viability assays. The cell density of the confluent wells was constantly between  $30,000 \pm 1200$  cells/cm<sup>2</sup> during the 10-day experimental protocol, which was confirmed each time by cell counting. There was a minor decrease (approximately 10%) in viability in response to pretreatment, then the switch to inductive conditions resulted in a significant loss of cells ( $p < 0.001$ ), but all of the remaining (approximately 40% of control) cells were vital, showing almost exclusively neural morphological characteristics. In the maturation phase, there was a

minor recovery in cell viability, but the number of viable cells was still significantly lower than it had been initially.

### 3.4. Changes in the expression of neuronal markers during induction

The time-dependent changes of neuronal marker gene expression in DPSC cultures undergoing neural development was evaluated by RT-PCR (Fig. 4). DPSCs isolated from five independent healthy human donors were subjected to our three step differentiation protocol. Total RNA was harvested at six different time points during this period: at time 0 (non-induced control DPSCs), after 2 days of pretreatment, on the first day of induction, on the third day of induction, after 24 h of maturation, and after 3 days of maturation.

Transcripts for mesenchymal vimentin, the neural progenitor marker nestin, the neuronal N-tubulin and NSE were already detectable in the non-induced and pretreated DPSCs, confirming the presence of neural progenitors in the mesenchymal fibroblastic cultures (Fig. 4A and B). During induction, NF-M was strongly expressed, while vimentin and nestin became downregulated. A transient decrease in N-tubulin expression was also observed (Fig. 4C and D). During the maturation phase, the glial marker GFAP became detectable, the neuronal NGN2 was strongly upregulated, NF-M was downregulated, while nestin and N-tubulin expression increased (Fig. 4E and F). NSE was present at every examined time

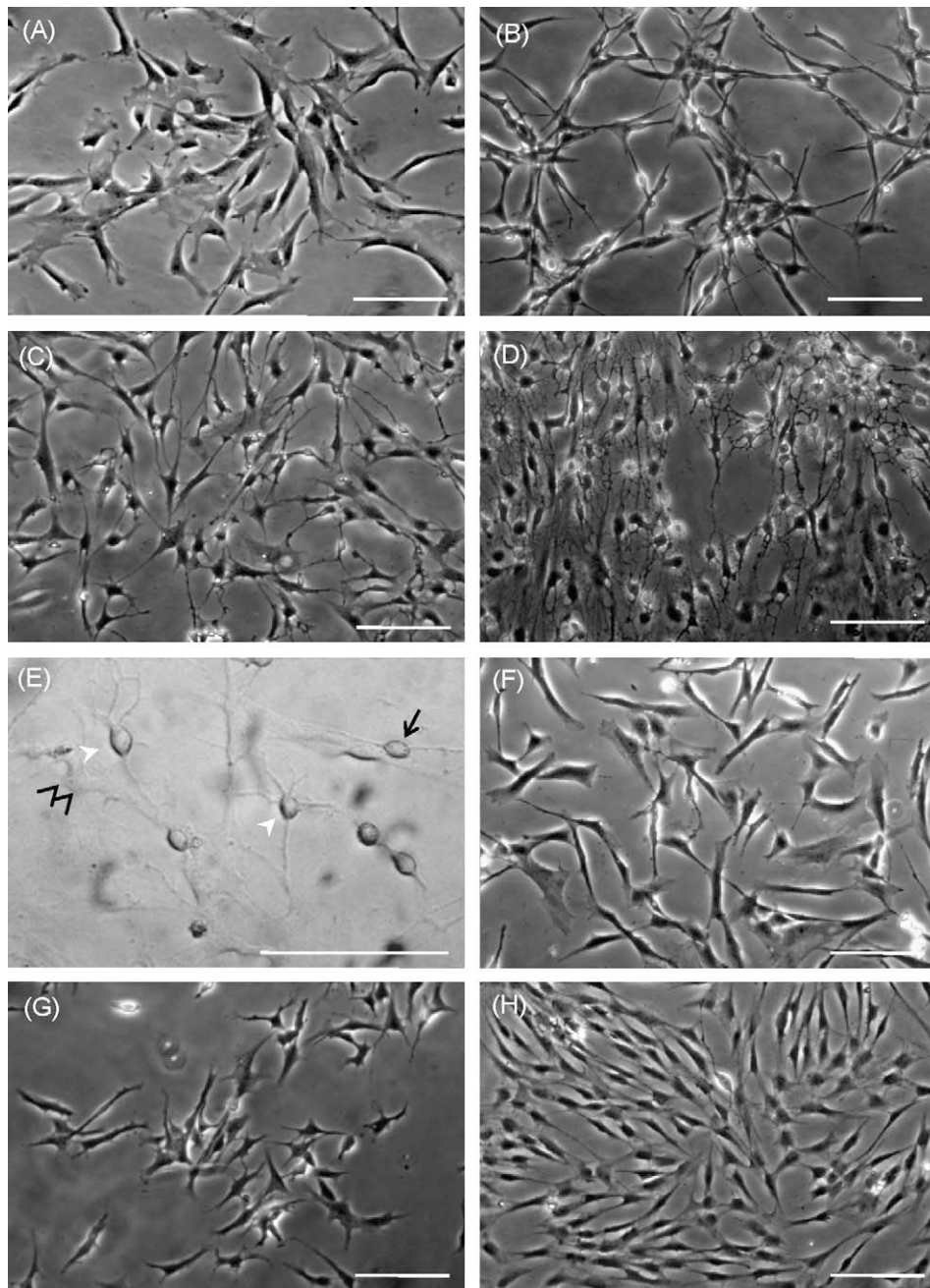


**Fig. 2.** Morphological changes during neuronal differentiation of DPSCs. (A) Control DPSCs had spindle-shaped morphology on poly-L-lysine coated plastic surface. (B) After 24 h of induction, cells formed clusters. (C) One day after the removal of the inductive medium, the aggregates spread, and most of the cells started to take a more spherical shape and developed extending processes. (D) After 3 days of maturation, cells had morphological features typical of neurons, showing complex neuronal processes. (E) After 10 days of differentiation, most of the cells displayed either multi- or bipolar forms (signed by the white arrowheads and the black arrow), while beneath them some flat cells were also observed (showed by the black arrowheads). (F) Omitting the intracellular cAMP increasing components, or (G) excluding the PKC activator TPA from the differentiation protocol resulted in the development of incomplete neural-like morphology by the 10th day of the differentiation procedure. (H) When applying a recently described differentiation protocol on DPSC cultures, originally developed for periodontal ligament derived culture (Widera et al., 2007), the proportion of cells displaying neuronal morphology compared to the entire population was very small. The lengths of the bars indicate 100  $\mu\text{m}$ .

point during differentiation, and its expression progressively increased under maturing conditions. As expected, expression of  $\beta$ -actin, which served as an endogenous control, was constant in all phases of differentiation.

To quantify the changes in the mRNA expression of neuronal marker genes at different time points, we performed real-time PCR assays (Fig. 5). The expression of each target gene was normalized to that of the RPLP0 housekeeping gene, and expressed as fold change relative to the non-induced sample. The decrease in the expression was sharp for vimentin and nestin, and moderate for N-

tubulin in response to neurogenic stimulation ( $p < 0.05$ ). The expression of NSE, NF-M and the glial intermediate filament GFAP increased during induction and maturation ( $p < 0.05$ ).

Immunocytochemical analysis was performed in the final maturation stage of the differentiation, to correlate with mRNA expression data. The protein expression pattern of the DPSCs fixed on the 10th day of neural differentiation showed a mixed population harboring neural cells expressing the early appearing neuronal microtubule marker N-tubulin, (Fig. 6A), intermediate filament subunit NF-M (Fig. 6B), the glial intermediate filament

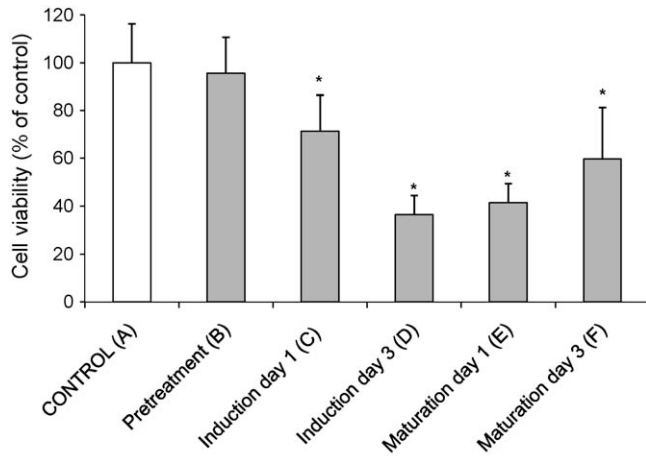


**Fig. 3.** Cell viability of DPSCs during the three step differentiation protocol, assessed by MTT assay. Data are reported as mean  $\pm$  S.E. in % of the untreated control ( $n = 4$ ). 48 h of 5-azacytidine-bFGF pretreatment had no effect on the number of living cells. On the contrary, by the end of the induction, less than 40% of the initial viable cells were detectable. Small elevation of the cell viability was observed during maturation. However, cell loss compared to initial value still remained significant (\*,  $P < 0.001$ , tested by one-way ANOVA, and post hoc Dunnett's test).

marker GFAP (Fig. 6C), or postmitotic nuclei protein NeuN (Fig. 6D). Control staining of non-induced DPSCs or differentiated DPSCs incubated without primary antibodies did not detect any specific staining (not shown). Expression of N-tubulin, NF-M and NeuN was observed in more than half of the neuronally committed DPSCs. On the contrary, immunostaining for glial specific markers was seen only on less than 10% of the cells.

### 3.5. Electrical properties of differentiated DPSCs

Membrane currents were measured to confirm that a subpopulation of dental pulp cells had the potential to develop into functionally active neuronal cells. Altogether five parallel DPSC cultures, differentiated for 8–11 days, were prepared for patch clamping. Fig. 7A shows the representative whole-cell current traces obtained by whole-cell clamping of a DPSC derived neural cell on the 10th day of differentiation, exhibiting typical multipolar neuronal morphology. The arrow with diamond indicates the voltage-activated sodium current  $I_{Na}$  (Fig. 7A), which was shown to be sensitive to 1 mM TTX (Fig. 7B). Circle indicates the delayed, outwardly rectifying potassium current  $K_{DR}$  (Fig. 7A), which was demonstrated to be sensitive to 5 mM TEA (Fig. 7C). The apparent inward  $Na^+$  current inactivated very rapidly, while the outward  $K^+$

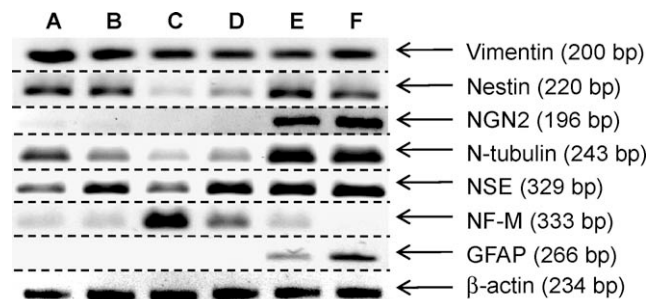


**Fig. 4.** Gene expression during neural differentiation of DPSCs, assessed by semi-quantitative RT-PCR as described in Section 2.  $\beta$ -Actin was used as an endogenous control in the experiments: (A) non-induced DPSCs, (B) after 2 days of pretreatment, (C) on the first day of induction, (D) on the third day of induction, (E) after 24 h in the maturation mixture and (F) after 3 days of maturation. Arrows indicate PCR products of the correct size for each amplicon.

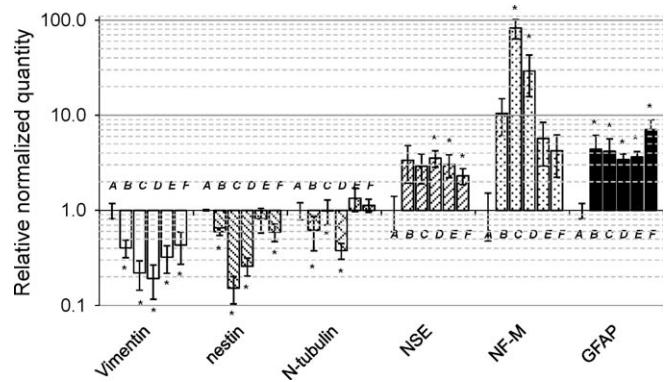


**Fig. 5.** mRNA expression pattern of mesenchymal, neuronal and glial markers in DPSCs during neuronal differentiation. Total RNA of DPSCs isolated from five independent normal human donors was used. RNA was harvested at six time points during the differentiation of each sample: from non-induced DPSCs (A), after 2 days pretreatment (B), on the first day of induction (C), on the third day of induction (D), after 24 h of maturation (E), and after 3 days of maturation (F). Target gene expressions were normalized to RPLP0 housekeeping gene expression levels and evaluated as fold change relative to the non-induced sample. mRNA expression of the mesenchymal vimentin and neural precursor nestin appeared to be significantly suppressed by the treatment, while the mRNA expression of the neuron specific glycolytic enolase NSE, neuronal intermediate filament medium polypeptide NF-M, and glial intermediate filament protein GFAP was significantly elevated by the stimulation. A minor temporal decrease in the expression level of the early appearing neuronal N-tubulin was observable, but its transcription increased during the maturation phase (\* indicates  $P < 0.05$ , calculated by one-way repeated measures of ANOVA and post hoc Dunnett's test). Data are reported as mean  $\pm$  S.E.

current was a delayed current, likely to be non-inactivating within the time of the test pulse 50 ms.

The amplitudes of  $K_{DR}$  were measured 40 ms after the onset of the pulse, while  $Na^+$  current amplitudes were detected at the peak values. After normalizing the currents with membrane capacities, three subsets of cells became separable. The first subpopulation ( $n = 5$ , type 1) displayed fast inactivating  $Na^+$  currents which were completely blocked by 1 mM TTX, with a threshold between  $-60$  and  $-50$  mV, and a maximum around  $-40.1 \pm 4.0$  pA/pF at  $-10$  mV (from a holding potential of  $-70$  mV, Fig. 7D). 1 mM TTX completely blocked the sodium currents of type 1 cells having neuronal morphology. Delayed, outwardly rectifying currents ( $K_{DR}$ ) were also demonstrated in these cells. 5 mM TEA partially reduced the  $K_{DR}$  currents (Fig. 7C). The threshold of the current was at  $-30$  mV, and the maximum current densities were around  $88.3 \pm 6.1$  pA/pF at  $+10$  mV (Fig. 7E). The passive membrane conductance in these cells was about  $1.7 \pm 0.4$  nS. Another subset of the cells (type 2,  $n = 21$ ) expressed TTX sensitive  $Na^+$  currents with the same threshold as observed in type 1 cells (Fig. 7D), but their maximal amplitudes were only about  $-19.0 \pm 5.1$  pA/pF around 0 mV.  $K_{DR}$  currents were observed after depolarization over a threshold of  $-30$  mV as seen in type 1 cells, but the maximal amplitudes were only  $60.8 \pm 9.8$  pA/pF (Fig. 7E). The inhibitory effect of TEA was less pronounced in type 2 cells than in type 1 ones. The passive membrane conductance was  $2.5 \pm 0.8$  nS. The third group of cells (type 3,  $n = 12$ ), as well as the non-induced DPSCs, displayed a passive membrane conductance of  $25 \pm 10.1$  nS, and did not exhibit any voltage dependent ion currents. However, in contrast to non-induced cells, they showed neuronal-like morphology.

## 4. Discussion

In the present work we describe for the first time that neural crest derived adult human dental pulp stem cells can be differentiated into cells that not only express several neural markers, but also simultaneously display voltage dependent sodium and potassium currents. We have developed a relatively

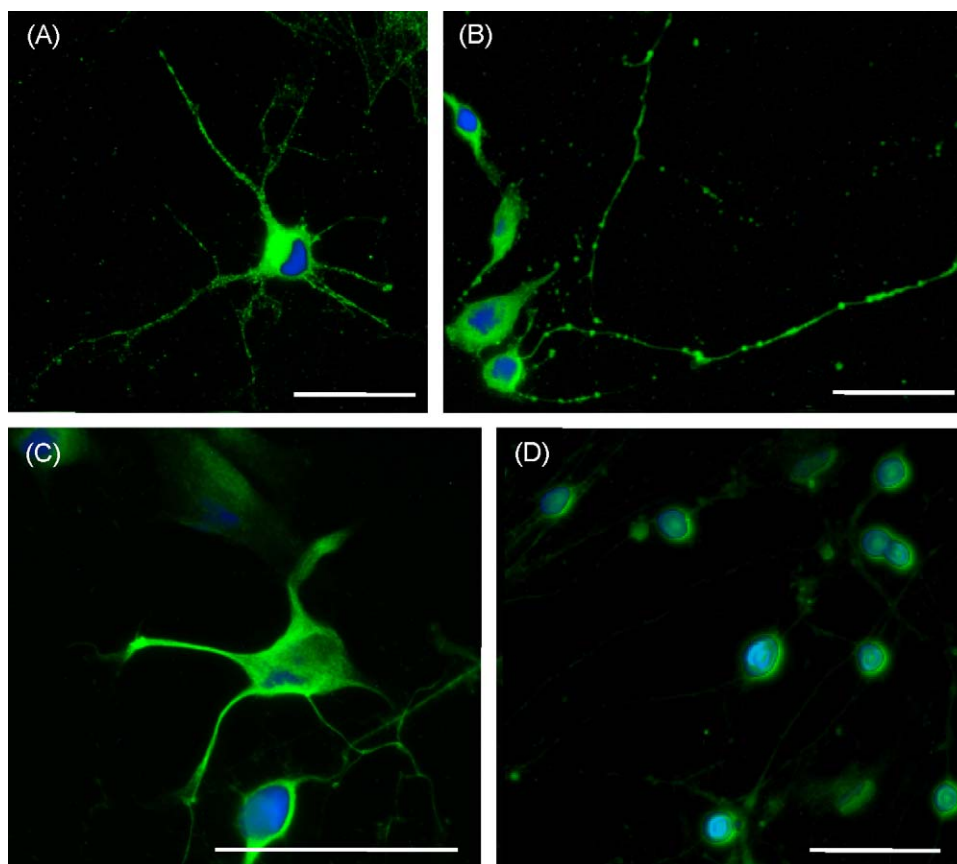


**Fig. 6.** DPSCs expressed neural markers after 10 days of differentiation: (A) neuron specific microtubule marker N-tubulin, (B) neuronal NF-M and (C) glial GFAP intermediate filament protein was primarily observed in the processes of cells. (D) NeuN neuronal nuclei protein was visible in some cell nuclei. Nuclei were visualized by DAPI. The lengths of the bars indicate 40  $\mu\text{m}$ .

rapid and highly reproducible differentiation protocol that selectively supports the development and survival of neural progenitor cells residing in dental pulp derived cultures. Our three step protocol is based on the combination of previously described treatments primarily applied to BMSC cultures, resulting in either temporal or long term expression of neural markers (Kohyama et al., 2001; Nagai et al., 2007; Scintu et al., 2006; Tataru et al., 2007; Widera et al., 2007). The complex stimulatory effect of our protocol involves the influence of 5-azacytidine on cell plasticity and neurogenesis, the inductive effect of the cross-talk between the protein kinase C and cyclic AMP pathways and the maturation inducing effect of the combination of known differentiation promoting agents. When applied to DPSCs, our protocol results in a mixture of immature and more mature neural cells, and presumably it does not support the survival of mesenchymal fibroblastic elements that have no potential for neural commitment. Beside the stimulatory agents, another important factor that might affect the efficiency of the differentiation is the plating cell density. In preliminary experiments when we used either higher or lower initial cell concentrations, we found that both the number of cell clusters formed during the induction and the proportion of cells growing neuronal processes under maturing conditions were considerably lower. Our observations are in line with previous data (Jelitai et al., 2007; Tarnok et al., 2002) showing that physical cell-to-cell contacts may be crucially important for neuronal commitment of DPSCs as well as of neural progenitor cells obtained from other tissue sources.

Our RT-PCR and real-time PCR results show that non-induced DPSCs already express neuronal markers such as nestin, N-tubulin and NSE, as well as low levels of NGN2 and NF-M. However, we

could not detect substantial expression of GFAP in these undifferentiated DPSC cells. These data indicate that already at the non-treated stage, at least a subset of DPSCs have high potential for neural differentiation. Following pretreatment and induction, vimentin and the progenitor marker nestin became downregulated. This phenomenon, in conjunction with cell viability data, suggests that stimulation of neural differentiation results in the loss of a large fraction of the cells, and at the same time triggers neurogenic mechanisms in the surviving population. This is supported by the time-dependent changes of expression of the intermediate/mature neural markers NSE and GFAP as their levels gradually elevated during the first two steps of the protocol, while NF-M expression dramatically increased during induction by combined PKC-cAMP activation. Only a small percentage of DPSCs started growing processes and developed neuronal morphology during the PKC-cAMP activation period suggesting that the visible changes in morphology occur much slower than the alterations in gene expression. Our data suggest that approximately 40% of the cells survive the combined, sustained activation of the PKC and cAMP systems. This level of cell loss is not surprising, considering that long term PKC activation results in cell proliferation arrest followed by programmed cell death, an effect that has been attributed to the PKC delta isoform (Racz et al., 2006). The c-kit stem/progenitor cell marker was previously shown to be expressed in about 20% in DPSC cultures without neurogenic induction (Laino et al., 2005). Only 5–10% of the cells in DPSC cultures were shown to be immunoreactive for STRO-1, another early mesenchymal stem cell marker (Shi and Gronthos, 2003). Therefore, the proportion of cells that survive the induction period is clearly much higher than that of the cell population that has progenitor

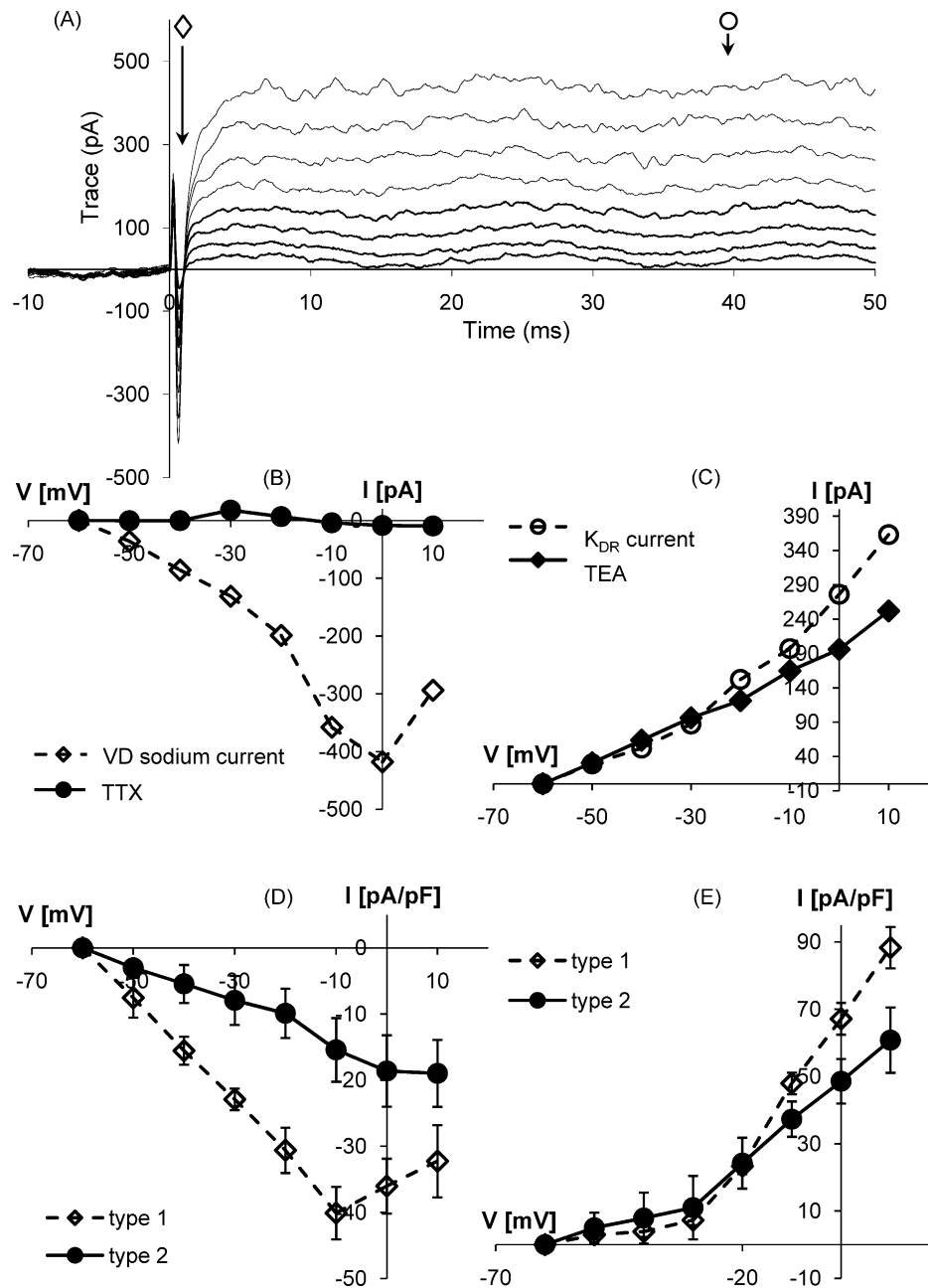


**Fig. 7.** Representative whole-cell recordings measured on a DPSC derived neuronal (type 1) cell showing typical multipolar neuronal morphology displayed voltage-activated sodium (diamond) and delayed outwardly rectifying potassium (circle) currents (A). (B) In some experiments, voltage gated sodium channels were blocked by TTX. (C)  $K_{DR}$  currents were partially TEA sensitive. (D and E)  $I-V$  relationship of voltage-dependent currents recorded on differentiated DPSCs. To normalize the measured currents for appropriate cell sizes, the changes in current amplitudes were expressed as changes in current densities (pA/pF). Five DPSC cultures collected from different hosts were used for electrophysiological measurements. By their  $I-V$  characteristics, cells could be divided into three basic groups: type 1 ( $n = 5$ ) showed mature, type 2 ( $n = 21$ ) produced voltage-gated currents with smaller amplitudes, type 3 ( $n = 12$ ) did not express any voltage-dependent ionic channels. Empty diamonds show the currents displayed by type 1, full circles indicate the data measured on type 2 cells. (D) TTX sensitive sodium currents. (E) TEA sensitive potassium currents. Data are reported as mean  $\pm$  S.E.

characteristics in the initial cell population. During maturation, the cell number only moderately increased, presumably due to limited cell proliferation. These data suggest that not only the subset of DPSCs originally expressing stem/progenitor markers has the capability of differentiating towards neural cells. Other cells of the DPSC cultures may also differentiate in response to the inductive treatment.

In the final maturation phase of the protocol described in the present study, the expression levels of N-tubulin, NSE, NGN-2 and GFAP increased, and NeuN immunoreactivity was also detected. Vimentin and nestin expression increased as well, but they did not increase over the initial levels measured in non-induced DPSCs.

The mRNA level of the late neuronal marker NF-M, which is known to be expressed prior to final maturation, decreased after peaking on the first day of induction. These data suggest that a fraction of induced cells entered the final developmental stage of neurogenesis. For the expression profile of these markers, similar observations were made previously (Arthur et al., 2008) using a fundamentally different protocol for neural differentiation.

In addition to mRNA and protein expression results, the characteristics of ion currents obtained by patch clamping indicate that the differentiation of adult human dental pulp cells results in the development of a mixed, heterogeneous cell population. Within this population are subsets that contain neurally com-

mitted cells in different proportions. Embryonic stem cell derived neural stem cells were shown to express voltage-sensitive sodium currents only after a few days' exposure to inductive media (Biella et al., 2007; Jelitai et al., 2007). The progressive increase of current amplitudes during neuronal maturation was documented by several studies (Biella et al., 2007; Jelitai et al., 2007; Okamura and Shidara, 1990; Takahashi and Okamura, 1998). Cells derived from neuronal regions of cleavage-arrested blastomeres isolated from ascidian embryos display different, altering types of voltage dependent sodium and potassium channels along the 80 h of the developmental period starting with the event of fertilization (Okamura and Shidara, 1990). The early voltage gated channel forms are gradually replaced over time with the more mature types. Our investigations indicate that a subset of differentiated DPSCs exhibits sodium currents displaying mature characteristics, while another subpopulation also exists among the differentiated DPSCs that displays premature currents. Therefore, subsets of differentiated DPSCs may represent distinct developmental stages. Taken together, the above-mentioned electrophysiological studies raise the possibility that distinct subtypes of sodium channels might be present in the membrane of differentiated DPSCs, but further investigations are necessary for their detailed characterization.

We observed similar heterogeneities among the amplitudes of the evaluated outward delayed rectifier potassium currents.  $K_{DR}$  currents are delayed potassium currents that play a major role in membrane repolarization during an action potential, and were reported to appear during neurogenesis prior to the expression of voltage dependent sodium currents (Biella et al., 2007; Jelitai et al., 2007; Takahashi and Okamura, 1998). Their density, as well as their TEA sensitivity, increases during maturation (Jelitai et al., 2007). Therefore, it may not be surprising that the subset of differentiated DPSCs displaying more mature, characteristic type of sodium currents, expressed  $K_{DR}$  currents with increased amplitudes and higher TEA sensitivity (type 1). On the other hand, the type 2 subpopulation exhibited a premature sodium current pattern, and produced  $K_{DR}$  currents with lower amplitudes and moderate TEA sensitivity. These data provide important additional functional evidence for the neuronal differentiation of human DPSCs. A very recent pioneer work reported that voltage dependent potassium currents could not be detected on DPSCs that underwent neuronal differentiation and displaying voltage gated sodium currents (Arthur et al., 2008). The reason for the discrepancy between the two studies is not clear, but it might be attributed to the different inductive protocols resulting in different levels of neuronal differentiation.

Another neuronal feature investigated on DPSCs by patch clamping was the passive conductance, which is known to be very small in maturing neurons (Jelitai et al., 2007). Passive membrane conductance values measured on type 1 and type 2 DPSCs were lower by one order of magnitude than those measured on type 3 cells. Although these cells had some morphological features typical of neurons, they did not produce any voltage dependent ion currents. These data suggest that type 3 DPSCs may have remained in an early progenitor stage, or are as yet undescribed, non-differentiated neuron-like fibroblastic byproducts of the differentiation process.

Overall, our observations confirm the presence of pluripotent cells in the adult dental pulp that can form both non-mesenchymal and mesenchymal derivatives. These results obtained in our *in vitro* multistep activation neurogenic model indicate that DPSCs may differentiate into cells with distinct neuronal phenotypes after exposure to specific signals and thus may help understand the molecular background of neuronal differentiation of adult neural progenitor cells. Eventually, these neurally committed DPSCs might represent a new, easily available pool for cell therapy of degenerative disorders of the central nervous system.

## Acknowledgements

This study was supported by the Hungarian Scientific Research Fund (OTKA 69008, 61543, 67250, 68940, 72385 and 79189) and the Medical Research Council (ETT 558/2006 and 145/2006). We thank Dr. Tamás Horváth for his help in statistical analysis and figure designation, and Dr. Gábor Rácz for his help during the preparation of the manuscript.

## References

- Allard, B., Magloire, H., Couble, M.L., Maurin, J.C., Bleicher, F., 2006. Voltage-gated sodium channels confer excitability to human odontoblasts: possible role in tooth pain transmission. *J. Biol. Chem.* 281, 29002–29010.
- Arthur, A., Rychkov, G., Shi, S., Koblar, S.A., Gronthos, S., 2008. Adult human dental pulp stem cells differentiate toward functionally active neurons under appropriate environmental cues. *Stem Cells* 26, 1787–1795.
- Audesirk, G., Cabell, L., Kern, M., 1997. Modulation of neurite branching by protein phosphorylation in cultured rat hippocampal neurons. *Brain Res. Dev. Brain Res.* 102, 247–260.
- Bang, Y.J., Pirnia, F., Fang, W.G., Kang, W.K., Sartor, O., Whitesell, L., Ha, M.J., Tsokos, M., Sheahan, M.D., Nguyen, P., Niklinski, W.T., Myers, C.E., Trepel, J.B., 1994. Terminal neuroendocrine differentiation of human prostate carcinoma cells in response to increased intracellular cyclic AMP. *Proc. Natl. Acad. Sci. U.S.A.* 91, 5330–5334.
- Biella, G., Di Febo, F., Goffredo, D., Moiana, A., Taglietti, V., Conti, L., Cattaneo, E., Toselli, M., 2007. Differentiating embryonic stem-derived neural stem cells show a maturation-dependent pattern of voltage-gated sodium current expression and graded action potentials. *Neuroscience* 149, 38–52.
- Bouchez, G., Sensebe, L., Vourc'h, P., Garreau, L., Bodard, S., Rico, A., Guilloteau, D., Charbord, P., Besnard, J.C., Chalon, S., 2008. Partial recovery of dopaminergic pathway after graft of adult mesenchymal stem cells in a rat model of Parkinson's disease. *Neurochem. Int.* 52, 1332–1342.
- Cabell, L., Audesirk, G., 1993. Effects of selective inhibition of protein kinase C, cyclic AMP-dependent protein kinase, and Ca(2+)-calmodulin-dependent protein kinase on neurite development in cultured rat hippocampal neurons. *Int. J. Dev. Neurosci.* 11, 357–368.
- Carles, G., Braguer, D., Dumontet, C., Bourgarel, V., Goncalves, A., Sarrazin, M., Rognoni, J.B., Briand, C., 1999. Differentiation of human colon cancer cells changes the expression of beta-tubulin isoforms and MAPs. *Br. J. Cancer* 80, 1162–1168.
- d'Aquino, R., Graziano, A., Sampaolesi, M., Laino, G., Pirozzi, G., De Rosa, A., Papaccio, G., 2007. Human postnatal dental pulp cells co-differentiate into osteoblasts and endothelial cells: a pivotal synergy leading to adult bone tissue formation. *Cell Death Differ.* 14, 1162–1171.
- Deng, W., Obrocka, M., Fischer, I., Prockop, D.J., 2001. *In vitro* differentiation of human marrow stromal cells into early progenitors of neural cells by conditions that increase intracellular cyclic AMP. *Biochem. Biophys. Res. Commun.* 282, 148–152.
- Ghosh, P., Singh, U.N., 1997. Intercellular communication in rapidly proliferating and differentiated C6 glioma cells in culture. *Cell Biol. Int.* 21, 551–557.
- Gronthos, S., Mankani, M., Brahimi, J., Robey, P.G., Shi, S., 2000. Postnatal human dental pulp stem cells (DPSCs) *in vitro* and *in vivo*. *Proc. Natl. Acad. Sci. U.S.A.* 97, 13625–13630.
- Hamanoue, M., Sato, K., Takamatsu, K., 2007. Inhibition of p38 mitogen-activated protein kinase-induced apoptosis in cultured mature oligodendrocytes using SB202190 and SB203580. *Neurochem. Int.* 51, 16–24.
- Hamill, O.P., Marty, A., Neher, E., Sakmann, B., Sigworth, F.J., 1981. Improved patch-clamp techniques for high-resolution current recording from cells and cell-free membrane patches. *Pflügers Arch.* 391, 85–100.
- Holliday, R., 1996. DNA methylation in eukaryotes: 20 years on. In: Russo, V.E.A., Martienssen, R.A., Riggs, A.D. (Eds.), *Epigenetic Mechanisms of Gene Regulation*. Harbor Laboratory Press, Cold Spring, pp. 5–27.
- Hung, S.C., Cheng, H., Pan, C.Y., Tsai, M.J., Kao, L.S., Ma, H.L., 2002. *In vitro* differentiation of size-sieved stem cells into electrically active neural cells. *Stem Cells* 20, 522–529.
- Iacovitti, L., Stull, N.D., Jin, H., 2001. Differentiation of human dopamine neurons from an embryonic carcinomal stem cell line. *Brain Res.* 912, 99–104.
- Jelitai, M., Anderova, M., Chvatal, A., Madarasz, E., 2007. Electrophysiological characterization of neural stem/progenitor cells during *in vitro* differentiation: study with an immortalized neuroectodermal cell line. *J. Neurosci. Res.* 85, 1606–1617.
- Kim, G., Choe, Y., Park, J., Cho, S., Kim, K., 2002. Activation of protein kinase A induces neuronal differentiation of HiB5 hippocampal progenitor cells. *Brain Res. Mol. Brain Res.* 109, 134–145.
- Kimiwada, T., Sakurai, M., Ohashi, H., Aoki, S., Tominaga, T., Wada, K., 2009. Clock genes regulate neurogenic transcription factors, including NeuroD1, and the neuronal differentiation of adult neural stem/progenitor cells. *Neurochem. Int.* 54, 277–285.
- Kohyama, J., Abe, H., Shimazaki, T., Koizumi, A., Nakashima, K., Gojo, S., Taga, T., Okano, H., Hata, J., Umezawa, A., 2001. Brain from bone: efficient "meta-differentiation" of marrow stroma-derived mature osteoblasts to neurons with Noggin or a demethylating agent. *Differentiation* 68, 235–244.

- Koyama, N., Okubo, Y., Nakao, K., Bessho, K., 2009. Evaluation of pluripotency in human dental pulp cells. *J. Oral Maxillofac. Surg.* 67, 501–506.
- Laino, G., d'Aquino, R., Graziano, A., Lanza, V., Carinci, F., Naro, F., Pirozzi, G., Papaccio, G., 2005. A new population of human adult dental pulp stem cells: a useful source of living autologous fibrous bone tissue (LAB). *J. Bone Miner. Res.* 20, 1394–1402.
- Ma, J., Wang, Y., Yang, J., Yang, M., Chang, K.A., Zhang, L., Jiang, F., Li, Y., Zhang, Z., Heo, C., Suh, Y.H., 2007. Treatment of hypoxic-ischemic encephalopathy in mouse by transplantation of embryonic stem cell-derived cells. *Neurochem. Int.* 51, 57–65.
- Magloire, H., Couble, M.L., Thivichon-Prince, B., Maurin, J.C., Bleicher, F., 2008. Odontoblast: a mechano-sensory cell. *J. Exp. Zool. B: Mol. Dev. Evol.*
- Magloire, H., Lesage, F., Couble, M.L., Lazdunski, M., Bleicher, F., 2003. Expression and localization of TREK-1 K<sup>+</sup> channels in human odontoblasts. *J. Dent. Res.* 82, 542–545.
- Miura, M., Gronthos, S., Zhao, M., Lu, B., Fisher, L.W., Robey, P.G., Shi, S., 2003. SHED: stem cells from human exfoliated deciduous teeth. *Proc. Natl. Acad. Sci. U.S.A.* 100, 5807–5812.
- Moore, K.D., Dillon-Carter, O., Conejero, C., Poltorak, M., Chedid, M., Tornatore, C., Freed, W.J., 1996. In vitro properties of a newly established medulloblastoma cell line MCD-1. *Mol. Chem. Neuropathol.* 29, 107–126.
- Nagai, A., Kim, W.K., Lee, H.J., Jeong, H.S., Kim, K.S., Hong, S.H., Park, I.H., Kim, S.U., 2007. Multilineage potential of stable human mesenchymal stem cell line derived from fetal marrow. *PLoS ONE* 2, e1272.
- Nosrat, I.V., Smith, C.A., Mullally, P., Olson, L., Nosrat, C.A., 2004. Dental pulp cells provide neurotrophic support for dopaminergic neurons and differentiate into neurons in vitro; implications for tissue engineering and repair in the nervous system. *Eur. J. Neurosci.* 19, 2388–2398.
- Okamura, Y., Shidara, M., 1990. Changes in sodium channels during neural differentiation in the isolated blastomere of the ascidian embryo. *J. Physiol.* 431, 39–74.
- Orojan, I., Bakota, L., Gulya, K., 2008. Trans-synaptic regulation of calmodulin gene expression after experimentally induced orofacial inflammation and subsequent corticosteroid treatment in the principal sensory and motor trigeminal nuclei of the rat. *Neurochem. Int.* 52, 265–271.
- Otte, A.P., van Run, P., Heideveld, M., van Driel, R., Durston, A.J., 1989. Neural induction is mediated by cross-talk between the protein kinase C and cyclic AMP pathways. *Cell* 58, 641–648.
- Pavlin, R., Kosir, N., Vidmar, V., 1991. Monoamine oxidase activity in rat and human odontoblasts: a microgasometric study. *J. Oral Pathol. Med.* 20, 200.
- Pavlin, R., Vidmar, V., 1979. Cholinesterases and choline acetylase in isolated human and rat odontoblasts. *Arch Oral Biol.* 24, 217–223.
- Racz, G.Z., Szucs, A., Szlavik, V., Vag, J., Burghardt, B., Elliott, A.C., Varga, G., 2006. Possible role of duration of PKC-induced ERK activation in the effects of agonists and phorbol esters on DNA synthesis in Panc-1 cells. *J. Cell Biochem.* 98, 1667–1680.
- Rizvanov, A.A., Kiyasov, A.P., Gaziziov, I.M., Yilmaz, T.S., Kaligin, M.S., Andreeva, D.I., Shafigullina, A.K., Guseva, D.S., Kiselev, S.L., Matin, K., Palotas, A., Islamov, R.R., 2008. Human umbilical cord blood cells transfected with VEGF and L(1)CAM do not differentiate into neurons but transform into vascular endothelial cells and secrete neuro-trophic factors to support neuro-genesis—a novel approach in stem cell therapy. *Neurochem. Int.* 53, 389–394.
- Schinstine, M., Iacovitti, L., 1997. 5-Azacytidine and BDNF enhance the maturation of neurons derived from EGF-generated neural stem cells. *Exp. Neurol.* 144, 315–325.
- Schroder, W., Hager, G., Kouprijanova, E., Weber, M., Schmitt, A.B., Seifert, G., Steinhauser, C., 1999. Lesion-induced changes of electrophysiological properties in astrocytes of the rat dentate gyrus. *Glia* 28, 166–174.
- Scintu, F., Reali, C., Pillai, R., Badiali, M., Sanna, M.A., Argioli, F., Ristaldi, M.S., Sogos, V., 2006. Differentiation of human bone marrow stem cells into cells with a neural phenotype: diverse effects of two specific treatments. *BMC Neurosci.* 7, 14.
- Sharma, S.K., Raj, A.B., 1987. Transient increase in intracellular concentration of adenosine 3':5'-cyclic monophosphate results in morphological and biochemical differentiation of C6 glioma cells in culture. *J. Neurosci. Res.* 17, 135–141.
- Shi, S., Bartold, P.M., Miura, M., Seo, B.M., Robey, P.G., Gronthos, S., 2005. The efficacy of mesenchymal stem cells to regenerate and repair dental structures. *Orthod. Craniofac. Res.* 8, 191–199.
- Shi, S., Gronthos, S., 2003. Perivascular niche of postnatal mesenchymal stem cells in human bone marrow and dental pulp. *J. Bone Miner. Res.* 18, 696–704.
- Song, L., Tuan, R.S., 2004. Transdifferentiation potential of human mesenchymal stem cells derived from bone marrow. *FASEB J.* 18, 980–982.
- Takahashi, K., Okamura, Y., 1998. Ion channels and early development of neural cells. *Physiol. Rev.* 78, 307–337.
- Tarnok, K., Pataki, A., Kovacs, J., Schlett, K., Madarasz, E., 2002. Stage-dependent effects of cell-to-cell connections on in vitro induced neurogenesis. *Eur. J. Cell Biol.* 81, 403–412.
- Tatard, V.M., D'Ipollito, G., Diabira, S., Valeyev, A., Hackman, J., McCarthy, M., Bouckenooghe, T., Menei, P., Montero-Menei, C.N., Schiller, P.C., 2007. Neurotrophin-directed differentiation of human adult marrow stromal cells to dopaminergic-like neurons. *Bone* 40, 360–373.
- Thesleff, I., Aberg, T., 1999. Molecular regulation of tooth development. *Bone* 25, 123–125.
- Tucker, A., Sharpe, P., 2004. The cutting-edge of mammalian development; how the embryo makes teeth. *Nat. Rev. Genet.* 5, 499–508.
- Widera, D., Grimm, W.D., Moebius, J.M., Mikenberg, I., Piechaczek, C., Gassmann, G., Wolff, N.A., Thevenod, F., Kaltschmidt, C., Kaltschmidt, B., 2007. Highly efficient neural differentiation of human somatic stem cells, isolated by minimally invasive periodontal surgery. *Stem Cells Dev.* 16, 447–460.